PROCEDURES USED TO ENSURE SUFFICIENT STRENGTH AND DAMPING IN HELICOPTER BEARINGLESS ROTORS

N.S. Pavlenko and A.Yu. Barinov

Mil Helicopter Plant
Moscow, Russia

Notation

$EIx_{1..3}$	flexible beam flapwise bending stiffness
$EIy_{1..3}$	flexible beam chordwise bending stiffness
Mx	flapwise bending moment
My	chordwise bending moment
Mz	torsional moment
Qy	flapwise force
Qx	chordwise force
N	centrifugal force
Cy	linear flapdwise stiffness
Cx	linear chordwise stiffness
$C\beta$	angular flapdwise stiffness
$C\xi$	angular chordwise stiffness
Ω	rotor rotational speed

Abstract

The paper presents analytical procedures used for determining the required damping as well as for calculating strength of the main structural members of helicopter bearingless rotors in different versions.

Analytical results obtained for damping ensured in the structure with the helicopter main rotor blade chordwise oscillations are given. The effect of the flexible beam shape on oscillation modes and load levels in the hub and blade is shown.

General Considerations Used in Designing Bearingless Rotors

The helicopter main rotor is one of the most complex components in the aircraft. Main rotor designing is a challenge involving the solution of a number of problems, such as aeroelastic stability, static strength, service life and technology.

In the last few decades intensive research on the development of bearingless rotors has been done. This design has been used successfully in many helicopters flying. A bearingless rotor is a rotor in whose design conventional hinges (flapping, lead-lag and feathering ones) are completely or partially eliminated. Blade flapwise and chordwise motions, as well as blade swaying about the longitudinal axis of the blade and blade pitch changes when collective and cyclic controls are applied are accomplished by elastic deformation of some structural member which is actually a flexible beam. At the same time, blade pitch changes and, sometimes, chordwise motion are ensured by elastomeric bearings. Elimination of rolling bearings and application of composite materials result in easier maintenance of rotors, more lightweight structures, longer service life and higher survivability.

Analytical Methods Used in Designing a Bearingless Main Rotor Hub.

Although there is a great variety of bearingless rotors in terms of their design, all of them have certain common members. Fig. 1 shows a schematic of the bearingless main rotor (BMR) design.
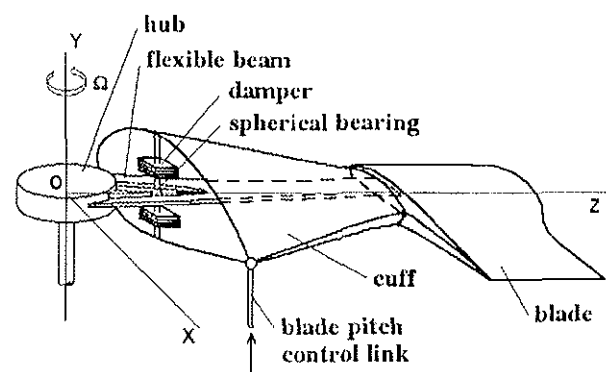
Fig. 1. Schematic of Bearingless Main Rotor.

The design consists of the hub to which the blade is attached by means of a beam flexible in bending and torsion. The blade pitch change is accomplished by a member rigid in bending and

torsion (cuff). The cuff via the elastomeric damper is carried by the spherical bearing which serves as a flapping hinge. Figs. 2 and 3 show the flexible beam deformation under loads applied to it and the cuff.
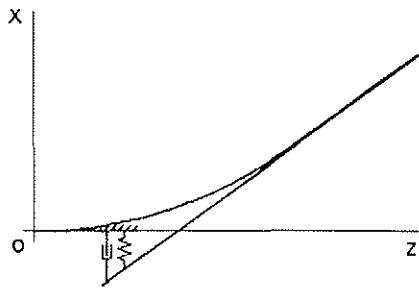
Fig. 2. Chordwise Deformation in Blade Root and Hub.
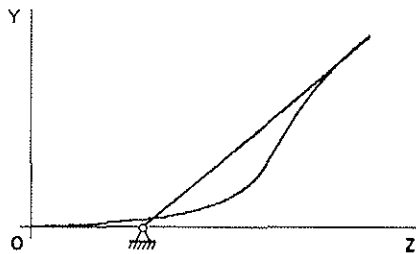
Fig. 3. Flapwise Deformation in Blade Root and Hub.

The hub sleeve and the root portion of the blade in different designs of the BMR can be presented by mechanical models as shown in Figs. 4-6.
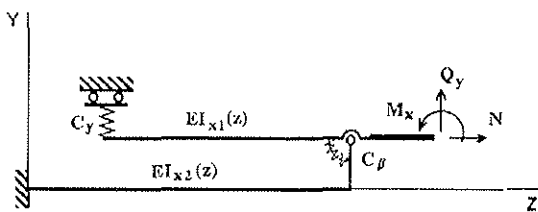
a. Flapwise
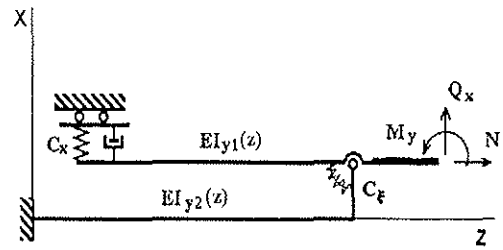
b. Chordwise

Fig. 4. Analytical Model of Hub Design. Version 1.
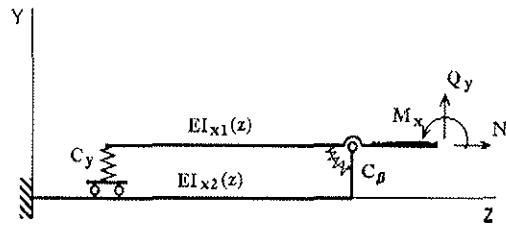
a. Flapwise
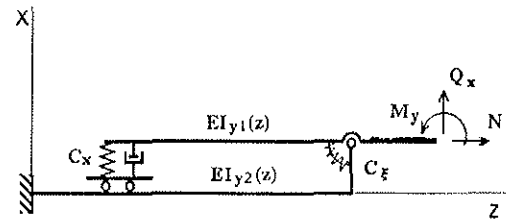
b. Chordwise

Fig. 5. Analytical Model of Hub Design. Version 2.
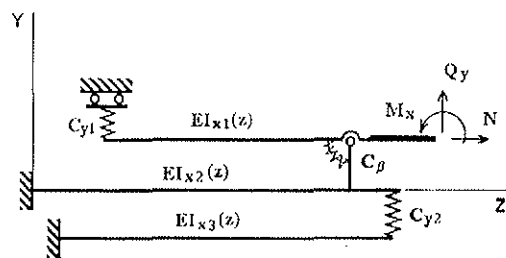
a. Flapwise
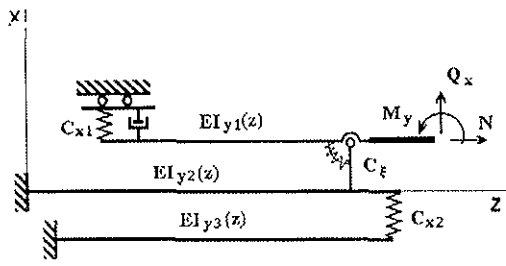
b. Chordwise

Fig. 6. Analytical Model of Hub Design. Version 3.

They present statically inderterminate bar systems. The centrifugal and shearing forces, and bending moments transmitted from the blade to the hub are denoted as N, Q_Y, Q_X, M_X, M_Y respectively. To determine inner force factors, acting in the hub components, the following method is used. The system of equations expressing a statically inderterminate system can be presented as follows:

$$A \bar{x} = B, \qquad (1)$$

where   A is a square matrix in which the a_{ij} elements are deflection caused by unit forces, $x_i=1$, acting in the direction of the x_j forces. Their values are defined from the well known formula:

$$a_{ij} = \int_l \frac{M_i M_j}{EI} dx \quad ;$$

where M_i and M_j are functions determining the values of the bar lengthwise bending moments,
EI is the bar rigidity in bending,
l is the bar length,
B is the column matrix of deflection caused by the ith -force factor acting in the direction of the jth force,
$\bar{x}$ is the column matrix of the unknowns whose number is equal to the order of statically inderterminate system (1).

The BMR hub design presented in Fig. 1 (as a schematic laoyut) and in Fig. 4-6 as mechanical models used for the analysis contains beams under tensile loads caused by the longitudinal (centrifugal) force. To determine the stress produced in these beams, we have to solve the following differential equation alongside system of equations (1).

$$EI\ q^{IV}-Nq^{II}=0 \qquad (2)$$

The solution of this equation has the following form:

$$q=C_1e^{kx}+C_2e^{-kx}+C_3x+C_4 \qquad (3)$$

Here C_i are unknown constants.

In the analysis the beam of variable cross-section is presented as a beam consisting of the n-segments of constant cross-section each. It is necessary to meet the boundary conditions for each segment. They have the following form for the inboard built-in segment:

$$q=0;$$
$$q^{I}=0.$$

As for the outboard free segment to which forces and moments are applied, the boundary conditions are as follows:

$$EIq^{III}-Nq^{I}=Q;$$
$$EIq^{II}=M.$$

Here   q is the generalized co-ordinate along which bending is considered. Besides, it is necessary to satisfy the conjugation conditions of adjacent segments loaded by concentrated forces and moments.

$$q_m(l_m)=q_{m+1}(0);$$
$$q^{I}_m(l_m)=q^{I}_{m+1}(0);$$
$$EI_m\ q^{II}_m(l_m)=EI_{m+1}\ q^{II}_{m+1}(0)+M_{m+1};$$
$$EI_i\ q^{III}_m(l_m)=EI_{m+1}\ q^{III}_{m+1}(0)-P_{m+1},$$

where l_m is the length of the m-th beam segment.

Thus we obtain a linear algebraic system of 4n equations containing unknown coefficients C_{lm} (m=1,z; l=1,4), that can be solved by using conventional mathematical means.By applying unit forces and moments to the end face of the analytical model presenting the main rotor hub (Fig. 4-6, right) and solving systems of equations (1) and (2), we obtain the matrix of rigidity for the hub sleeve at its attachment point to the blade.

$$C = \begin{vmatrix} C_{XX} & C_{XX'} & C_{XY} & C_{XY'} & C_{X\Phi} \\ C_{X'X} & C_{X'X'} & C_{X'Y} & C_{X'Y'} & C_{X'\Phi} \\ C_{YX} & C_{YX'} & C_{YY} & C_{YY'} & C_{Y\Phi} \\ C_{Y'X} & C_{Y'X'} & C_{Y'Y} & C_{Y'Y'} & C_{Y'\Phi} \\ C_{\Phi X} & C_{\Phi X'} & C_{\Phi Y} & C_{\Phi Y'} & C_{\Phi\Phi} \end{vmatrix}$$

Each matrix element $C_{q_k q_a}$ is stress produced in the direction of the q_k-th force factor during unit deflection in the q_a direction. The respective forces and moments at the blade root (where the blade is attached to the hub) can be calculated by using the following formula:

$$F = C \cdot \bar{q},$$

where

$$F = \begin{vmatrix} Q_X \\ M_Y \\ Q_Y \\ M_X \\ M_Z \end{vmatrix} \qquad q = \begin{vmatrix} x \\ x' \\ y \\ y' \\ \varphi \end{vmatrix}$$

x and x' are chordwise linear and angular hub deflection at the blade-to-hub attachment,

y and y' are flapwise linear and angular hub deflection,

and φ is the blade torsional deflection.

The rigidity matrix obtained in this case is used for analysing blade natural and forced oscillations.

When analysing forced oscillations, the blade is presented as finite elements with discrete parameters. Aerodynamic forces are calculated by using the lift coefficient, drag and torque as functions of the blade airfoil angle of attack and Mach number obtained from the wind tunnel results (Ref 3).

Analysis Used to Obtain Relative Damping for Blade Chordwise Oscillations.

To eliminate aeroelastic and mechanical instability of rotor oscillations, it is necessary to provide a sufficient level of damping for blade chordwise oscillations. From Fig 2 it can be seen that the damper works at cuff displacements relative to the hub (see also Fig 1). To calculate rotor blade damping, we can use a model of a viscoelastic body shown in Fig 7 (Ref 1).
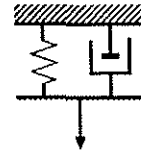
Fig. 7. Model of Viscoelastic Body.

The coefficient of oscillatory energy absorption is defined in the following expression:

$$\Psi = \frac{E_n}{E_P}, \qquad (4)$$

where E_n is the energy absorbed by the damper,
E_p is the kinetic energy produced by the blade motion.
Let us consider a linear damper; for it

$$M_D = k \cdot \dot{\xi} \qquad (5)$$

Here M_D is the damper moment,
k is the proportionality factor,
and ξ is the angular velocity of blade chordwise oscillations.
The energy absorbed by the damper during a period of oscillations $T = 2\pi$ can be defined as

$$E_n = \int_0^T M_D \, d\xi \qquad (6)$$

By substituting the damper moment from equation (5) in equation (6) and proceeding from the assumption that

$$\xi = \xi_0 \cdot \sin pt,$$

after simple transformations we obtain

$$E_n = \pi \, k \, \xi_0^2 \, p \qquad (7)$$

Here p is the oscillation frequency equal to the main rotor angular velocity.
The kinetic energy of blade oscillations in the first mode is defined by the formula:

$$E_p = \frac{1}{2} p^2 \sum_{i=1}^{zl} m_i x_i^2 \qquad (8)$$

where x_i is the first mode of natural oscillations,
zl is the number of elements into which the blade is divided in the analysis,
m_i is the mass of the i-th element.
By making substitutions (7) and (8) in (4),

we obtain:

$$\Psi = \frac{2\pi k \xi^2}{p \sum\limits_{i=1}^{zi} m_i x_i^2} \qquad (9)$$

Dynamic stiffness of a single-mass oscillatory system can be expressed as (Ref 2):

$$c_v = -mp^2 + iph_e + c_1,$$

where   m is the mass,
           p is the oscillation frequency,
           h_e is a damping coefficient,
           c_1 is the system spring rate
           and i is an imaginary unit.
           Fig 8 shows this value in the vector form.
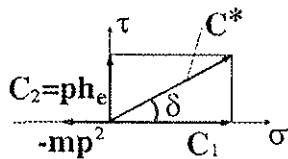
Fig. 8. Vector Diagram of Dynamic Stiffness.

Damper stiffness can be defined through a tangent of the loss angle:

$$c_2 = c_1 tg\delta \qquad (10)$$

The relative damping coefficient is derived from the following formula (Ref 2):

$$\bar{n} = \frac{\Psi}{4\pi} \qquad (11)$$

After substituting the expressions for Ψ and c2 from (9) and (10) respectively in equation (11), we finally obtain

$$\bar{n} = \frac{tg\delta \, c_2 \, \xi^2}{2 \, p^2 \sum\limits_{i=1}^{zi} m_i x_i^2} \qquad (12)$$

Let us replace angular displacements of the damper by linear ones in expression (12).

A linear displacement of the damper can be expressed in terms of an angular displacement as follows:

$$\Delta x = ltg\xi \approx l\xi,$$

where   l is the distance from the damper to the equivalent lead-lag damper.
Then we obtain

$$\bar{n} = \frac{tg\delta \cdot c_2^{lin} \cdot \Delta x^2}{2p^2 \sum\limits_{i=1}^{z} mx_i^2}$$

Let us determine the required volume of rubber in an elastomeris damper. The load applied to the damper is equal to

$$F = C_2^{lin} \Delta x \qquad (13)$$
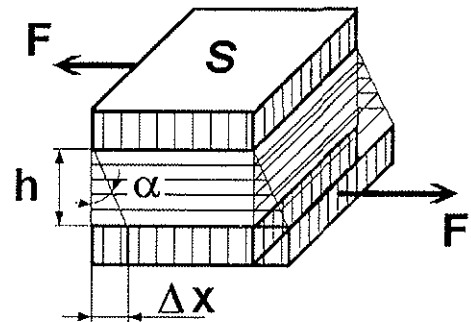
Fig. 9. Schematic of Elastomeric Damper Deformation.

The load equals the resistance of the damper rubber pack (Fig 9).

$$F_p = \tau S$$

Here τ is the shearing stress in the rubber pack and S is the shearing area.

$$\tau = G \cdot \alpha$$

where   G is the shearing modulus.

$$F_p = G\alpha S \qquad (14)$$

Equating expression (13) to expression (14), we obtain

$$G\alpha S = C_2^{lin} \Delta x$$

From which

$$C_2^{lin} = \frac{G\alpha S}{\Delta x} = \frac{GS}{h}$$

Thus, the required value of stiffness in the formula for relative damping is defined by linear dimensions of the rubber pack and the rubber stiffness.

Analytical Results.

Some results of the rotor damping analysis, as well as the structural analysis of the flexible beam made for an experimental bearingless main rotor intended for a light helicopter are given below (Fig. 10).
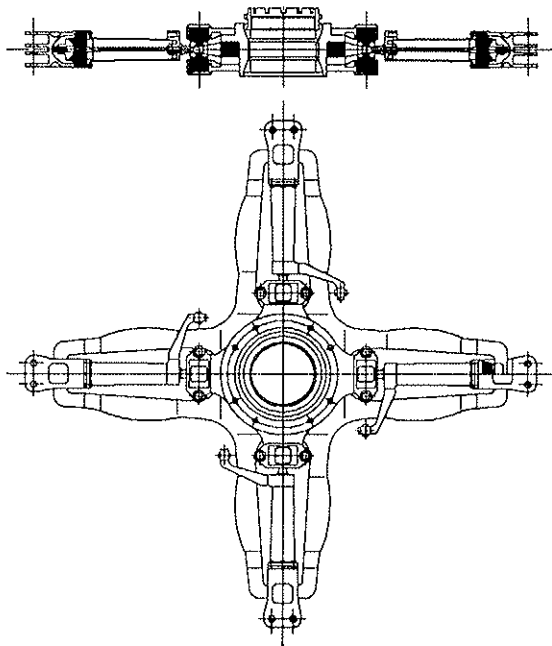
Fig. 10. Experimental Bearingless Rotor Hub.

The most critical member in the structure of a bearingless rotor from the point of view of its function is the flexible beam made either of an alloy or a composite material (see Figs 1 and 10). Its elastic properties determine, to a large extent, blade flapping, hub moment value, and, therefore, helicopter handling qualities, i.e. maneuverability and controllability. At the same time it is the most highly loaded structural member.

In this connection, a problem of selecting

flexible beam design parameters (from the point of view of its geometry and rigidity) arises because these parameters will greatly affect deflection levels, constant and alternating stresses in the flexible beam and the blade. The hub strength is determined by the loads applied in main flight conditions and during parking.

To find the algorithm for calculating the strength of the flexible beam during the process of design parametric analysis is a multistep task.

The first step is to calculate the deformation and constant stresses produced by the centrifugal force and blade droop caused by gravity during parking. The stresses produced by the blade droop can achieve quite a great value thus necessitating an introduction of special devices (blade droop stops) which make the design more complicated and result in a weight penalty. Therefore, it is desirable to eliminate them. It can be done by increasing the hub sleeve flapwise rigidity in bending. However, the increased rigidity results in a rise of in-flight alternating bending stresses defining the rotor service life.

The second step in the parametric analysis is to calculate alternating stresses by using the above mentioned procedures. Thus, the requirements for rigidity of the hub sleeve and blade root are essentially contradictory and they are a typical optimization problem.
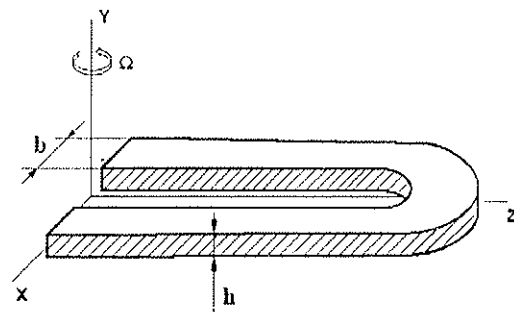
Fig. 11. Initial Configuration of Flexible Beam.

Fig 11 presents the initial configuration of the flexible beam taken from a drawing made at the initial stage of the hub designing (Fig 10).

Figs 12 and 13 show the lengthwise distribution of thickness and width of the flexible beam for the initial design.
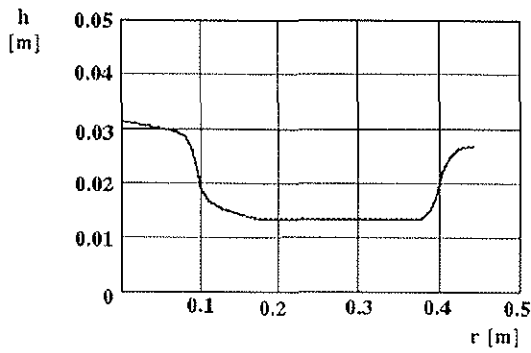
Fig. 12. Lengthwise Distribution of Initial Beam Thickness.
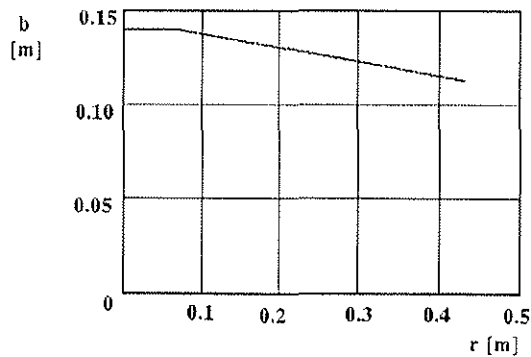
Fig. 13. Lengthwise Distribution of Initial Beam Width.

The estimated value of the equivalent chordwise alternating stresses in the beam was equal to $\sigma_y=11$ kg/mm². It is quite a challenge to achieve an acceptable service life for composite materials.

The in-plane equivalent alternating stresses in the beam turned out to be $\sigma_x=0.4$ kg/mm².
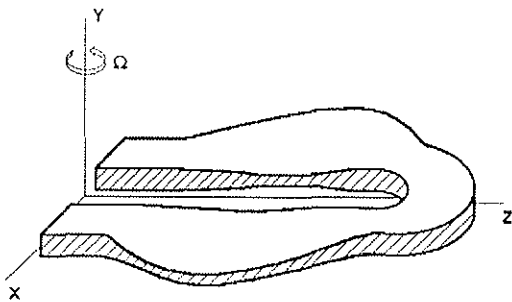
Fig. 14. Beam Configuration after Optimization.

The calculations made by using the above mentioned procedures allowed us to obtain the beam configuration shown in Fig 14. Figs 15 and 16 present the beam lengthwise distribution of thickness and width.
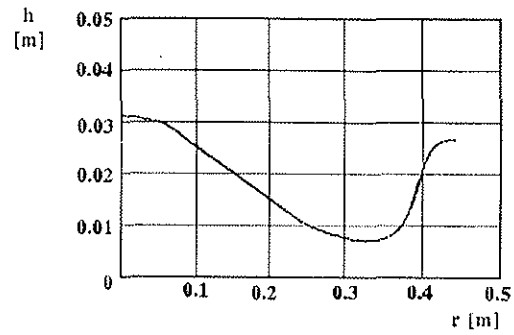
Fig. 15. Lengthwise Distribution of Beam Optimized Thickness.
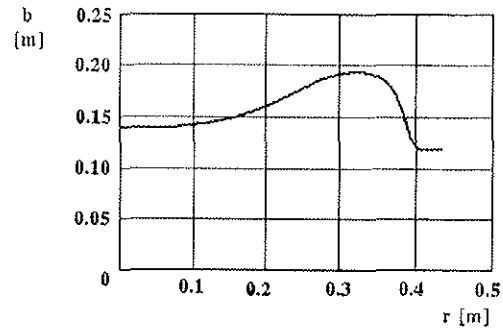
Fig. 16. Lengthwise Distribution of Beam Optimized Width.

The flap and in-plane equivalent stresses were $\sigma_y=6$ kg/mm² and $\sigma_x=0.3$ kg/mm² respectively. At the same time, the stresses produced by the blade droop decreased. Quite a long service life can be achieved for structures having equivalent stresses of this order.

Fig. 17 shows the relative damping coefficient versus stiffness of the damper; the data were obtained by using the above analytical procedures.
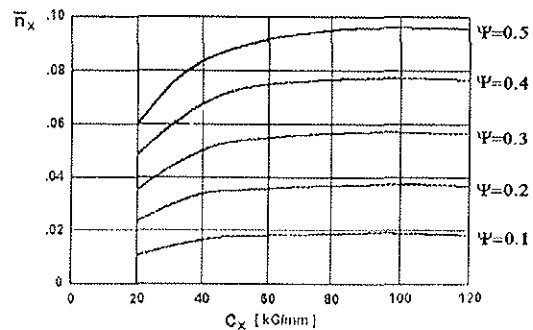
Fig. 17. Relative Damping Coefficient Versus Damper Stiffness.

The diagram in Fig 18 was plotted to define the damper optimal stiffness.
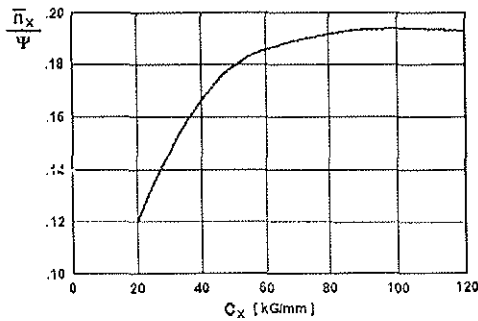
Fig. 18. Relative Damping Versus Damper Stiffness.

It can be seen from the diagram, that maximum damping is obtained for stiffness equal to 100 kg/mm. Fig. 19 shows the blade relative chordwise natural frequency when oscillating in the first mode versus the damper stiffness.
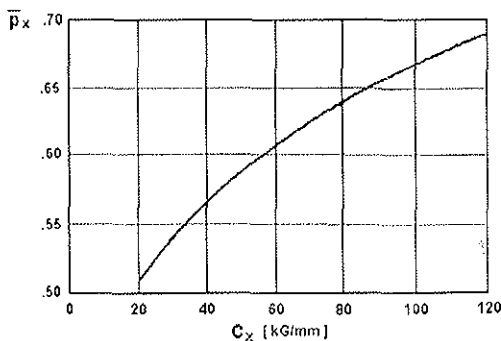
Fig. 19. Blade Relative Chordwise Natural Frequency Versus Damper Stiffness.

Proceeding from the analytical results, the damper stiffness was chosen to be equal to 100 kg/mm with the values of $\bar{p}_{x1}$ and $\bar{n}_x$ being 0.67 and 0.035 respectively for $\Psi=0.2$.

The damping value obtained is sufficient for eliminating all kinds of aeroelastic and mechanical instability.

Insufficient blade chordwise damping can lead to grave consequences.

This is how the main rotor hub incorporating a torsion strap pack has been developed for the Mi-34. Elastomeric dampers were to suppress blade chordwise oscillations. The damper design and the properties of rubber used there allowed us to obtain the following relative damping coefficient:

$$\bar{n}_x \cong 0.015 \div 0.02$$

During flight tests in some flight conditions the blade chordwise loads recorded revealed the presence of the blade natural frequencies which was a sign of an insufficient level of damping.

In addition, there was a strong blade torsional-chordwise oscillation coupling. The flight and ground tests conducted later revealed this coupling (Fig 20).
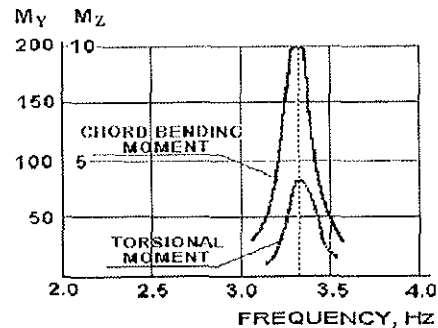
Fig. 20. Chordwise Bending and Torsional Moments Versus Frequency for a Hub Incorporating Elastomeric Dampers.

A low level of chordwise damping and the presence of coupling of the blade chordwise and control system oscillations caused instability of blade-control system oscillatons in one of the test flights.

This required a modification of the main rotor hub. Hydraulic dampers were installed alongside the elastomeric ones. Their installation increased the relative chordwise damping coefficient up to $n_x=0.08-0.12$. The mode of the blade and control system oscillations was also changed. It can be seen from Fig 21 that there is no coupling of blade chordwise bending with torsion in the modified hub. Further flight testing revealed that the helicopter was free from the instability found out earlier.
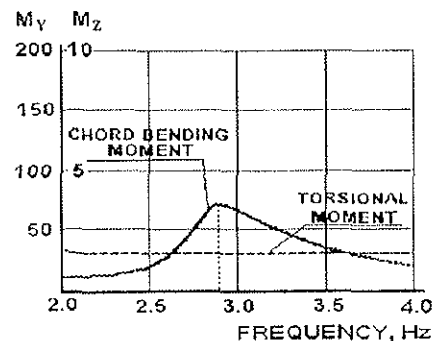
Fig. 21. Chordwise Bending and Torsional Moments Versus Frequency for a Hub Incorporating Elastomeric and Hydraulic Dampers.

When the tests were completed, the Mi-34 helicopter was certified and put in production.

References

1. Пановко Я.Г. Внутреннее трение при колебаниях упругих систем. Москва, Физматгиз, 1960. 193 с.

2. Вибрации в технике. Т.1. Под. ред. В.В.Болотина. Москва, "Машиностроение", 1978. 352 с.

3. Pavlenko N.S., Barinov A.Yu.: "Analysis of Torsional Moments Produced in Main Rotor Blades and Results Obtained," Proceedings of the Twenty First European Rotocraft Forum, Saint-Petersburg, Aug.-Sept. 1995.